

A charge-transfer resistance model and Arrhenius activation analysis for hydrogen ion transmission across single-layer graphene

*Saheed Bukola and Stephen E. Creager**

Department of Chemistry, Clemson University, Clemson SC 29634

KEYWORDS:

Graphene, 2D materials, proton transmission, Nafion, hydrogen pumping.

ABSTRACT

Transmission rates for protons and deuterons across single-layer graphene embedded in Nafion | graphene | Nafion sandwich structures are measured as a function of temperature in electrochemical hydrogen pump cells. Rates of ion transmission through graphene are obtained in the form of area-normalized ion-transfer resistances, and are interpreted in terms of ion-exchange current densities and standard heterogeneous ion-transfer rate constants. An encounter pre-equilibrium model for the ion-transfer step is then used to provide rate constants for the fundamental microscopic step of ion (proton or deuteron) transmission across graphene.

Application of this rate model to interpret variable-temperature data on proton and deuteron transmission rates provides values for the activation energy and pre-exponential factor for the fundamental ion transmission step across graphene. Activation energies obtained from the Arrhenius plots for proton and deuteron transmission are as follows; for proton, $E_{\text{act}} = 48 \pm 2 \text{ kJ mole}^{-1}$ ($0.50 \pm 0.02 \text{ eV}$) and for deuteron, $E_{\text{act}} = 53 \pm 5 \text{ kJ mole}^{-1}$ ($0.55 \pm 0.05 \text{ eV}$). The difference between these two values of approximately 5 kJ mole^{-1} is in good agreement with the expected difference in vibrational zero-point energies for O-H and O-D bonds, albeit with some uncertainty given the uncertainties in the activation energy values. Pre-exponential frequency factor values of $8.3 \pm 0.4 \times 10^{13} \text{ s}^{-1}$ and $4.7 \pm 0.5 \times 10^{13} \text{ s}^{-1}$ were obtained for proton and deuteron transmission respectively across graphene. These pre-factor values are both quite large, on the order of the values predicted from the Eyring – Polanyi equation with a transmission coefficient near one. The ratio of 1.8 for the rate pre-factors (H/D) is in reasonable agreement with the value of 1.3 for the ratio of bond vibrational frequencies for O-H and O-D stretching, respectively. Taken together, these data support a model in which proton and deuteron transmission across graphene are largely adiabatic processes for which the differences in transmission rate at room temperature are due largely to differences in activation energies.

1.0 Introduction.

Pristine graphene has long been thought of as a near-perfect barrier material, blocking transmission of all species having electron clouds surrounding atomic nuclei and forming molecular bonds.[1, 2] As an example, transmission of helium atoms at high pressure is reported to be completely blocked by a pristine piece of single-layer graphene covering a hole through which the helium could otherwise pass.[2, 3] Proton transmission is especially interesting because in the absence of solvent, the proton is unique among chemical species in that it is a nuclear particle with no electron cloud. It could at least in principle pass through a graphene sheet without an accompanying electron cloud. In fact, multiple recent reports have now appeared confirming room-temperature proton transmission through single-layer graphene at high rates.[4-9] Deuteron transmission also occurs at high rates, albeit not as high as protons.[4, 6, 7] These findings are possible only if activation energies for proton and deuteron transmission through graphene are much lower than has been predicted from a wide range of computational studies.[10-15] A fully satisfying explanation for these observations of high-rate proton / deuteron transmission through graphene has not yet been given. One possibility is that protons pass through defect sites that are rare, and spectroscopically undetected.[8, 14, 16] If defect sites are involved, they must be of a type that can allow for hydrogen ion transmission at very high rates, with significant isotopic selectivity, while blocking all other ions. Hydrogenated[16] and/or hydroxylated[8] defects, and atom placement defects such as Stone-Wales defects,[14] are candidate structures that have been considered as sites for enhanced proton transmission. Another possibility is that protons may be transmitted directly through graphene without the requirement of a structural defect site. This highly intriguing possibility will require more work

to confirm, but if true, it would significantly change the thinking about graphene as a barrier material.

We recently reported on the use of electrochemical hydrogen pump cells to study proton and deuteron transmission through single-layer CVD graphene in Nafion | graphene | Nafion sandwich structures.[4] Electrochemical hydrogen pump cells consist of a pair of electrodes that are catalytic for both the hydrogen reduction reaction (HRR) and the hydrogen evolution reaction (HER), separated by a proton-conducting electrolyte. Application of a potential difference between the electrodes then leads to hydrogen oxidation at one electrode and reduction at the other, with proton transmission occurring between the electrodes, across the electrolyte. The net effect is then electrochemical pumping of hydrogen gas from one side of the cell to another. Our recently published work utilized electrodes consisting of platinum nanoparticles supported on carbon black (Pt-on-carbon), and proton-conducting electrolytes consisting of Nafion 211 membranes. Pt-on-carbon electrodes were supported on carbon cloth and were hot-pressed onto the Nafion membrane prior to study, and graphene layers were positioned between two Nafion membranes also using a hot-press technique. Cell resistance is obtained from the slope of a current-voltage curve acquired using slow-scan cyclic voltammetry. Ion currents in excess of one A cm^{-2} were reported in such cells for proton transmission at bias voltages of just a few hundred millivolts. Other ions, e.g. potassium, are transmitted at much lower rates, possibly consistent with a defect mechanism for those ions. These very high ion currents for hydrogen isotope transmission through graphene mandate a low activation energy for proton / deuteron transmission through graphene as noted above, however in our prior work we did not acquire the variable-temperature rate data that would be needed for an Arrhenius activation analysis. Such an

analysis would provide activation energies and other rate parameters that could lend insight into the mechanism by which proton / deuteron transmission through graphene occurs.

The present work reports variable-temperature measurements of proton and deuteron transmission through single-layer graphene in Nafion | graphene | Nafion sandwich structures. The data are interpreted via a model that treats proton and deuteron transmission as an interfacial charge-transfer reaction that may be described via a heterogeneous ion-transfer rate constant and a first-order rate constant for transmission of ions poised at a reaction plane near the graphene surface. This treatment allows for an Arrhenius analysis of the proton / deuteron transmission rate constants that provides values for both the activation energies and the pre-exponential frequency factors associated with the fundamental microscopic step of proton and deuteron transmission through graphene. The findings lend important insight into the reaction pathways and mechanisms that might be operative to allow for high-rate hydrogen ion transmission through graphene.

2.0 Experimental.

2.1 Materials. Chemical vapor deposition (CVD) single-layer graphene on copper foil was obtained from ACS Materials, LLC. Nafion[®]-211 membranes were obtained from the Fuel Cell Store. Platinized carbon cloth and titanium mesh gas diffusion electrodes used to fabricate the membrane electrode assemblies (MEA) were purchased from the Fuel Cell Store. Hydrogen gas (Ultra high purity-200) and deuterium gas (Research grade) were provided by Airgas from large cylinders, connected through gas lines to the cell apparatus. Gas humidification was

accomplished by bubbling the gas through a temperature-controlled gas bubbler containing H₂O or D₂O. Gas flow rates were set using rotameters (from Dwyer) that were set at 0.02 SLM.

2.2 Nafion | graphene | Nafion fabrication and MEA assembly. Figure 1 illustrates the procedural steps involved in the making of Nafion | graphene | Nafion sandwich MEAs, which are similar to those disclosed in our recent prior work.[4] A square of CVD graphene on Cu (2.0 x 2.0 cm) was cut and placed on top of a Nafion[®]-211 membrane disk (19.1 mm diameter) that was supported by Teflon-reinforced fiberglass. This assembly was hot pressed together in a Carver hot press at 140 °C, 600 lb_f, for 2 min. Thereafter, the underlying Cu was removed in an etching solution of 0.3M (NH₄)₂S₂O₈ in water, leaving behind a single layer of graphene on the Nafion[®] membrane. After a thorough rinse in water, a second piece of Nafion[®] membrane was hot pressed on top of the graphene-on-Nafion at 140 °C again at 600 lb_f, for 2 min to make the Nafion | graphene | Nafion sandwich. This step may sometimes be combined with the MEA assembly. Next, two platinized carbon cloth electrodes (0.3 mg Pt cm⁻²) of size 3/16 inch (4.76 mm) diameter were cut using an arch punch. Next, 1 μL 5 wt. % Nafion[®] solution was added to these electrodes and allowed to dry. The electrodes were then hot pressed together onto either side of the Nafion membrane sandwich structures, with and without single layer graphene, again at 140 °C, 600 lb_f, for 5 min.

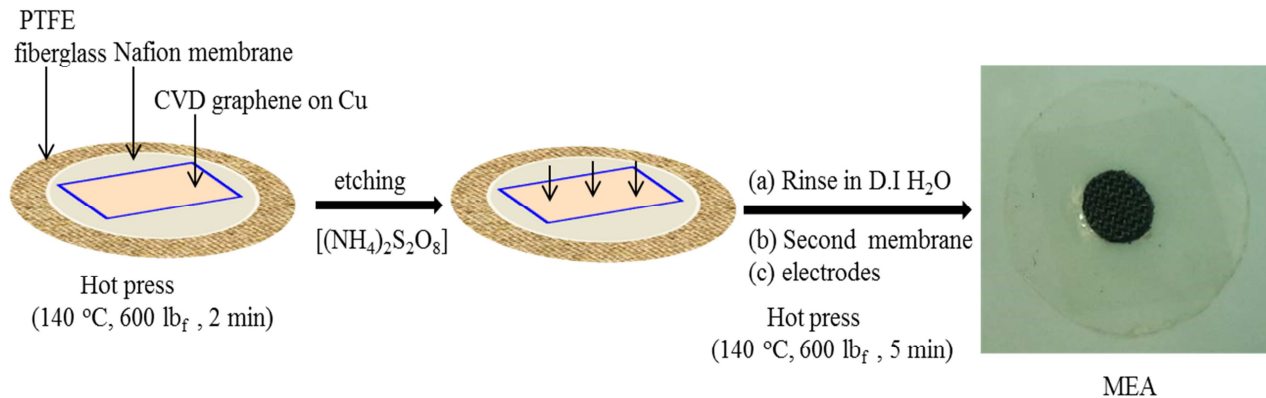


Figure 1. Schematic illustrations for the fabrication of Nafion | graphene | Nafion sandwich structure and the making of MEA. The photomicrograph at the right hand side is the completed MEA that shows graphene sandwiched between the Nafion[®] membranes visible to the eye.

MEA characterization data provided in our recent prior report are relevant to this report since MEA fabrication methods are the same. The recent prior report includes Raman spectra and graphene defect count measurements by an etch / visualization method.[4]

2.3 Electrochemical measurements. The variable-temperature cell used during this study has been described in details in reference 4. In brief, the cell body is made from a ¾-inch-diameter stainless-steel compression fitting, the current collectors were made of titanium rod and titanium meshes were used as gas diffusion layers, to enable better temperature control compared to earlier versions of the cell that used plastic parts. Electrochemical hydrogen pump experiments were performed in symmetric mode whereby both sides of the cell (anode and cathode) were bathed with humidified hydrogen or deuterium gas. The Nafion membranes were treated prior use and were converted to proton form and deuterium form by immersion in 1M H₂SO₄ or 1M D₂SO₄ respectively, followed by rinse in H₂O and D₂O respectively. Cell testing was performed at 30, 40, 50 and 60 °C. Two independently prepared MEAs were tested for each hydrogen pump

experiment with and without single layer graphene, and similarly for deuterium pump experiments. Current-potential (IV) curves were acquired using a CH Instruments model 1140B potentiostat in linear sweep voltammetry mode. Scan rate was 0.001 V s^{-1} for all symmetric hydrogen and deuterium pump experiments.

3.0 Results and Discussion

3.1 Variable-temperature measurement of proton and deuteron transmission through single-layer graphene. Figure 2 presents a schematic diagram of the cell and the membrane-electrode assemblies (MEA) that were used to perform these studies. MEA fabrication was accomplished as described above and in our recent prior work.[4, 17] In brief, a sample of CVD single-layer graphene on copper foil is hot-pressed onto a $\frac{3}{4}$ -inch-diameter Nafion 211 membrane, then the copper is removed by an ammonium persulfate oxidative etch, then a second Nafion 211 membrane disk is added via a second hot-press step. Following conversion of the MEA to the proton form by soaking in aqueous sulfuric acid, electrode disks consisting of platinum-on-carbon coated onto carbon cloth are added to each side of the MEA in a third hot-press step. (Sometimes the second and third hot-press steps are combined.) The MEA is then mounted in a cell consisting of a Swage-style compression fitting, adapted to accommodate a pair of current collector rods with holes drilled in them to carry humidified hydrogen gas to and from MEA. The cell is similar to that used in our recent prior work[4, 17] except that the cell body is made of stainless steel and the current collector rods are made of titanium metal. The use of metal components allows for better heat conduction and more reliable temperature control. The same sequence of steps is followed for studying deuteron transmission except that water is replaced by D_2O , sulfuric acid is replaced by D_2SO_4 , and hydrogen gas is replaced by deuterium gas. Further details are provided in the supplemental materials and in our prior published work.[4, 17]

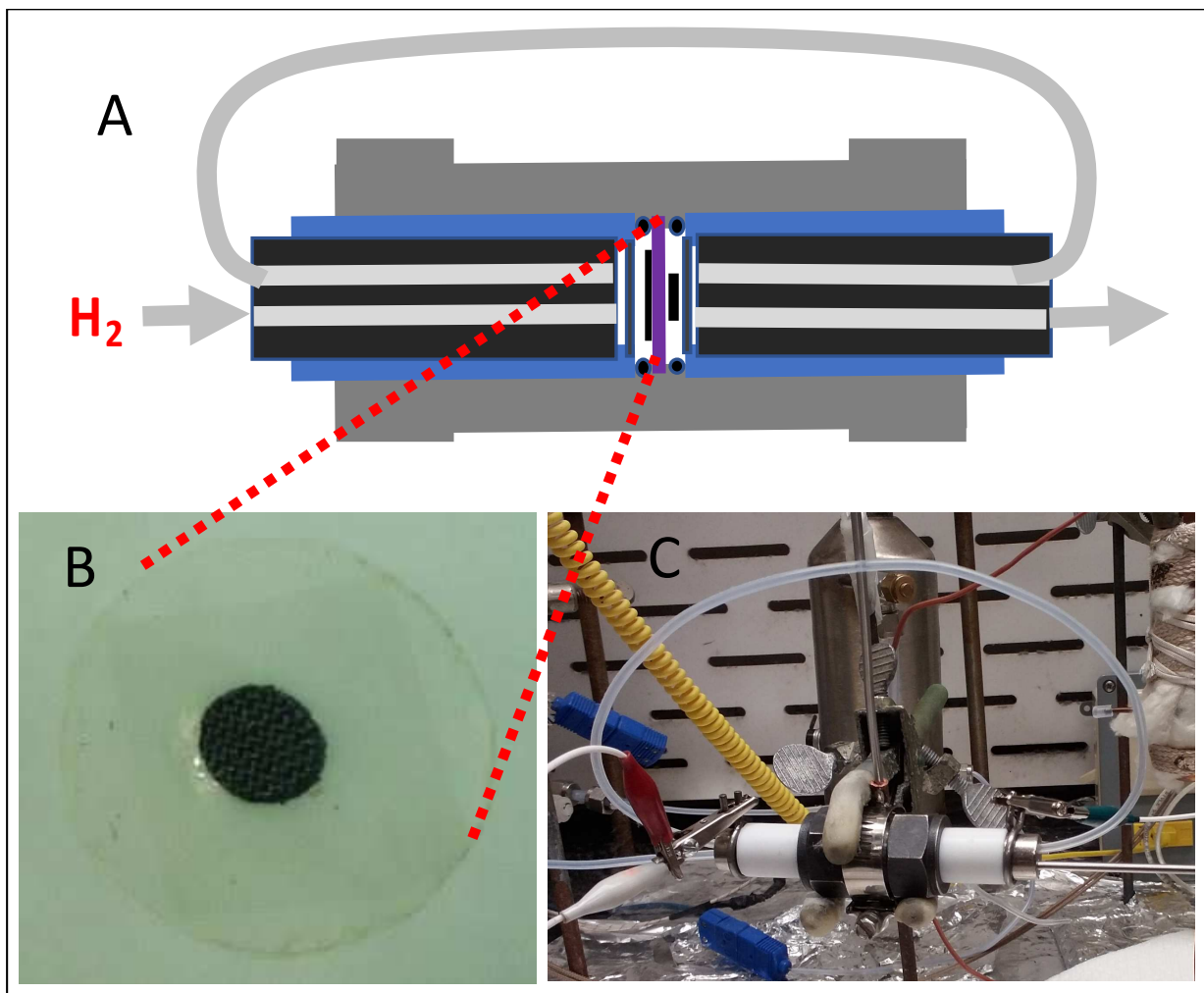


Figure 2. Illustrations of the electrochemical hydrogen pump cell and membrane-electrode assemblies (MEA) used for proton / deuteron transmission studies. (A) Schematic diagram of the cell configuration showing hydrogen gas entry and exit ports, and placement of the MEA inside the cell. (B) Photomicrograph of a completed MEA. Nafion membrane diameter = 3/4 inch (19.1 mm), electrode diameter = 3/16 inch (4.76 mm), electrochemically active area = 0.178 cm². The rectangular portion of graphene sandwiched between the Nafion membranes is visible in this micrograph. (C) Photograph of the cell in operation.

Figure 3 presents representative current-voltage (IV) curves for Nafion sandwich MEAs with and without graphene, for proton and deuteron transmission at variable temperature. (IV curves for all MEAs including duplicate runs for each MEA type and temperature are included in the Supplemental Materials.) The IV curve slopes all increase with increased temperature, as expected for a thermally activated process. In the cells without graphene, the slopes for deuteron transmission through Nafion are only slightly lower than those for proton transmission, consistent with the expectation that proton and deuteron transport are almost equally kinetically facile in hydrated Nafion membranes. This finding may reflect the fact that the species being transported are H_3O^+ and D_3O^+ respectively, for which the molecular masses are 19 and 22 Daltons. The heavier homologue is expected to move more slowly through the Nafion matrix, as is observed. The IV curves for cells with graphene confirm the observation reported previously that proton currents are almost unattenuated by graphene whereas deuteron currents are substantially attenuated.[4, 6, 7] Our previous study showed that the same Nafion | graphene | Nafion cells that pass proton currents at high rates, show potassium ion currents that are many orders of magnitude smaller.[4] This finding strongly indicates that the large proton currents are not a consequence of macroscopic physical defect sites that would allow any ion to pass. Proton and deuteron transmission must happen at sites that do not allow any other ions to pass at significant rates.

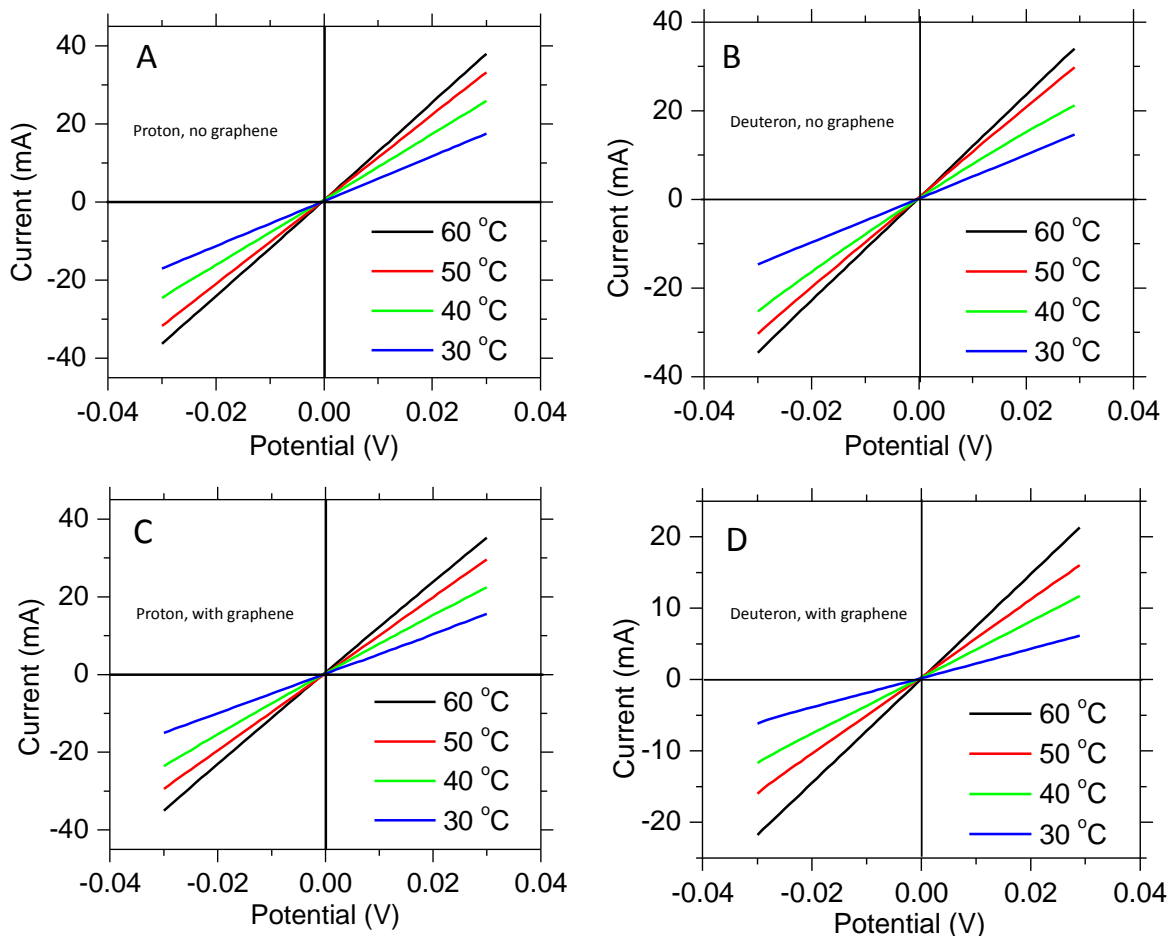


Figure 3. Representative current-voltage (IV) curves acquired in hydrogen-pump cells for proton and deuteron transmission, using Nafion sandwich MEAs with and without graphene. (A), proton, no graphene; (B), deuteron, no graphene; (C), proton, with graphene; (D) deuteron, with graphene. Note the different current scale for D. Scans were acquired at a potential scan rate of 0.001 V s^{-1} .

Table 1 presents a summary of data from all the IV curves, reported as MEA resistances (inverse slopes of IV curves). For each membrane type and each temperature, the measurement was made twice, once on each of two independently-prepared MEAs, and the Table reports the

average and standard deviation of the two measurements. (All the original data and the resistances for each membrane and temperature are reported in the Supplemental Materials.) The resistance data are further analyzed by subtracting the resistance for cells without graphene from that for cells with graphene, to obtain the series resistance contribution of graphene to the overall cell resistance. Resistance values for graphene alone are then reported as areal resistances by multiplying resistance by active area. Uncertainty in the graphene areal resistance values is calculated by propagating the uncertainty from the measured resistances with and without graphene into the calculated difference resistance for just the graphene.

Table 1. Cell resistance and rate parameters for proton and deuteron transmission through Nafion sandwich membranes with and without graphene.

Proton							
T	Ravg without graphene	Ravg with graphene	Rgraphene	Rgraphene * area	I0	ko	kPT
C	ohm	ohm	ohm	ohm cm2	amp cm-2	cm s-1	s-1
30	1.726 ± 0.003	1.949 ± 0.024	0.215 ± 0.024	0.038 ± 0.004	0.658	4.24E-03	4.24E+05
40	1.188 ± 0.006	1.320 ± 0.023	0.132 ± 0.024	0.023 ± 0.004	1.148	7.39E-03	7.39E+05
50	0.924 ± 0.002	1.004 ± 0.016	0.080 ± 0.016	0.014 ± 0.003	1.955	1.26E-02	1.26E+06
60	0.811 ± 0.005	0.854 ± 0.001	0.043 ± 0.005	0.008 ± 0.001	3.749	2.41E-02	2.41E+06
Deuteron							
30	1.988 ± 0.039	5.05 ± 0.27	3.062 ± 0.273	0.545 ± 0.049	0.048	3.09E-04	3.09E+04
40	1.225 ± 0.056	2.503 ± 0.051	1.278 ± 0.076	0.227 ± 0.013	0.119	7.64E-04	7.64E+04
50	0.977 ± 0.009	1.829 ± 0.034	0.852 ± 0.035	0.152 ± 0.006	0.184	1.18E-03	1.18E+05
60	0.851 ± 0.014	1.326 ± 0.061	0.475 ± 0.063	0.085 ± 0.011	0.339	2.19E-03	2.19E+05

It is interesting to note that uncertainties in cell resistance are quite low for studies of proton transmission through Nafion alone but are significantly larger for deuteron transmission through Nafion alone, and for both proton and deuteron transmission through Nafion containing graphene. The higher uncertainty for deuteron transmission through Nafion alone could reflect the presence of traces of protons in the D₂O used in deuteron transmission. It would be easy for the D₂O to become contaminated with traces of H₂O when working in a lab containing a lot of

water, and the higher transmission rate for protons relative to deuterons means that small amounts of H₂O could have a large effect. Measurement uncertainty in cells with graphene may reflect a contribution from structural defects in the graphene, which could vary from cell to cell. Even with these uncertainties, the relative uncertainties in the cell resistances are nearly always less than five percent, and those in the graphene resistances that are calculated by difference are all less than 20 percent.

3.2 Analysis of ion transmission rate data via a charge-transfer resistance model. A deeper analysis of the ion transmission rate data is possible by considering the graphene areal resistance as a charge-transfer resistance for protons (and deuterons), which may in turn be expressed as an exchange current density using equation 1 below.[18]

$$\frac{1}{R_{CT}} = \frac{\Delta i}{\Delta \eta} = i_0 \frac{F}{RT} \quad (1)$$

In this equation R_{CT} is the area-normalized charge-transfer resistance, $\Delta i/\Delta \eta$ is the slope of the IV curve, i_0 is the exchange current density for ion transmission, and F, R and T have their usual meaning. Exchange current densities for ion transmission may then be converted to standard heterogeneous ion-transfer rate constants, k^0 , in units of cm s^{-1} , using Equation 2.[18]

$$i_0 = Fk^0 C_{H^+} \quad (2)$$

In this equation, C_{H^+} is the concentration of ions (protons, deuterons) in the bulk Nafion phase at the reaction zone adjacent to the graphene surface. A value for C_{H^+} is obtained as the product of the ion-exchange capacity of the Nafion ionomer, which is 0.91 meq g⁻¹ for the 1100 equivalent weight material used in this work, and the specific gravity of Nafion in the protonated

/ deuterated form, taken as the literature value of 1.77 g cm^{-3} provided by Oberbroeckling and co-workers.[19] The values obtained for standard heterogeneous ion-transfer rate constants, reported in Table 1, are reasonable, and well within the range of values predicted by Marcus in his review on the application of Marcus theories of charge transfer to the case of ion transmission across boundaries between immiscible electrolytes.[20]

Finally, the standard heterogeneous ion-transfer rate constants may be converted to first-order ion-exchange rate constants, k_{PT} , in units of s^{-1} , via equation 3.[21]

$$k^0 = K_p k_{PT} = \delta \exp\left[\frac{-w_p}{RT}\right] k_{PT} \quad (3)$$

In this equation, K_p is the equilibrium constant for formation of the precursor complex from which ion transfer occurs, k_{PT} is the rate constant for ion transmission from the precursor complex across graphene, w_p is the average free energy required to transport the proton / deuteron reactant from the Nafion bulk to the reaction layer, and δ is the thickness of the reaction layer. For the present work we take w_p to be zero and δ to be one Angstrom unit, or 10^{-8} cm , following literature precedent from prior work applying this precursor model to the case of heterogeneous electron transfer at electrodes.[21] Table 1 lists values for proton / deuteron exchange rate constants for proton and deuteron transmission through graphene for the four temperatures studied in this work.

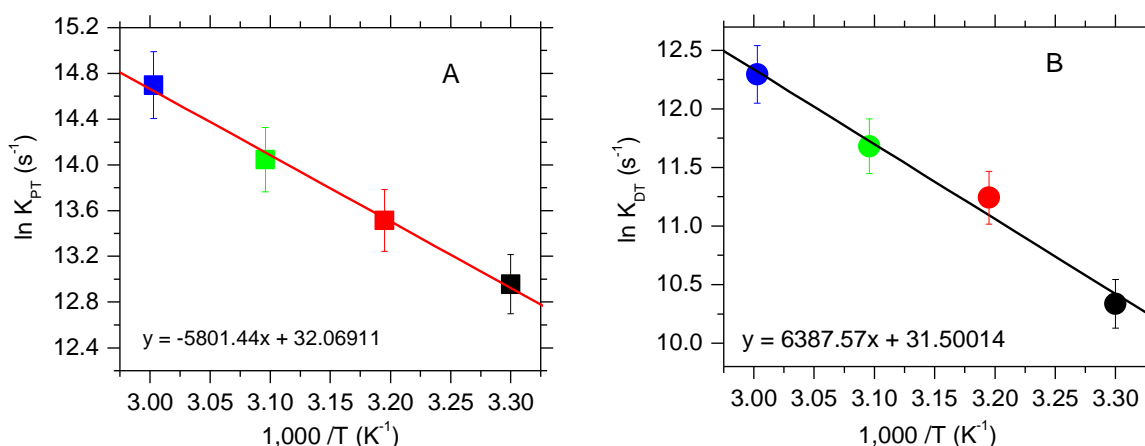


Figure 4 Arrhenius plots of proton exchange rate constants for (A) proton transmission and (B) deuteron transmission through single-layer graphene in Nafion | graphene | Nafion sandwich cells.

3.3. Arrhenius analysis of proton / deuteron transmission across graphene. Figure 4 presents Arrhenius plots of the proton exchange rate constants for proton and deuteron transmission through graphene, from Table 1. Both plots are linear over the temperature range studied which strongly indicates that proton and deuteron transmission through graphene are thermally-activated processes, in agreement with prior work.[5] From the slopes and intercepts of the plots we obtain the following activation energies E_{act} and frequency pre-factors A for proton and deuteron transmission; for proton transmission, $E_{act} = 48 \pm 2$ kJ/mole (0.50 ± 0.05 eV) and A is $8.3 \pm 0.4 \times 10^{13} \text{ s}^{-1}$, and for deuteron transmission, $E_{act} = 53 \pm 5$ kJ/mole (0.55 ± 0.05 eV) and A is $4.7 \pm 0.5 \times 10^{13} \text{ s}^{-1}$. Both activation energy values are slightly lower than the value of 0.78 ± 0.03 eV reported by Hu and co-workers in their 2014 report on proton transport through one-atom-thick crystals.[5] The low activation energies are consistent with the observation of high-rate hydrogen ion transmission at room temperature and are much lower than expected from a

wide range of computational studies on proton transmission through graphene, which predict activation energies that are nearly always well in excess of 1 eV.[8, 10-15] The discrepancy between theory and experiment on this issue remains unresolved. The difference between proton and deuteron transmission activation energies is approximately 5 kJ/mole or 0.05 eV which is close to the expected value of between 5 and 6 kJ/mole for the difference in vibrational zero-point energies for O-H and O-D vibrations.[22, 23] This difference in zero-point energies is the root cause of primary kinetic isotope effects in chemical reactions involving bond breaking / formation with protons.[24] The present findings are consistent with a mechanism whereby the different transmission rates for proton and deuteron are caused principally by the differences in activation energy for proton transmission, although, this conclusion must be interpreted with caution given the uncertainties associated with the Arrhenius plot slopes. An improved study would have to include many more data points than we were able to obtain, to reduce these uncertainties. The present findings are also consistent with the recent prior reports from Lozada-Hidalgo and co-workers which also found a difference of 0.06 eV for proton and deuteron transmission activation energies, albeit from studies at only a single temperature.[6, 7] The activation pre-factors were not explicitly addressed in that work, so the difference in activation energies was obtained from the difference in rates by assuming equal pre-factors for proton and deuteron transmission.

The absolute magnitudes of the pre-exponential frequency factors reported here for H^+ and D^+ transmission through graphene are possible because a specific rate model was adopted to interpret the graphene proton and deuteron areal resistances. It is instructive to consider the absolute magnitudes of these frequency factors in the context of simple theories. The Eyring–Polanyi equation predicts that pre-exponential frequency factors for thermally activated reactions

should be on the order of $\kappa k_B T/h$, where κ is the transmission coefficient which in simple terms is a probability of reaction from a system poised at the activated complex,[25] and k_B , T and h have their usual meaning. For an assumed value for κ of one and a temperature of 300K, this equation gives a pre-factor value of $6.2 \times 10^{12} \text{ s}^{-1}$, which is of the same order of magnitude, albeit somewhat lower than both of the experimentally obtained values reported above. The fact that the experimental frequency factor values obtained in this work are so large suggests that the proton transmission reaction across graphene may be largely adiabatic, with a transmission coefficient near 1.

The Eyring–Polanyi equation does not predict a difference in frequency factor values for proton and deuteron transmission. To address this issue, we consider the experimental values in terms of the vibrational frequencies for O-H and O-D bonds. The symmetric stretch vibration for H_2O occurs as a broad band centered at 3400 cm^{-1} , whereas that for D_2O is a similar broad band centered at 2500 cm^{-1} . [26, 27] Converting these values to bond vibrational frequencies leads to values of $1.0 \times 10^{14} \text{ s}^{-1}$ and $7.5 \times 10^{13} \text{ s}^{-1}$ for O-H and O-D stretching respectively. Similar results are obtained when considering O-H and O-D stretching in H_3O^+ and D_3O^+ . [28] These bond vibrational frequencies are also of the same order of magnitude as the experimentally observed Arrhenius frequency factors, albeit slightly larger. The ratio of 1.8 for the experimental pre-exponential frequency factors for proton and deuteron transmission is in reasonably good agreement with the ratio of 1.3 for the O-H and O-D vibrational bond frequencies. This finding is consistent with a model whereby the proton/deuteron transmission reactions follow a reaction coordinate that involves significant O-H and O-D bond stretching. The fact that the experimental pre-exponential frequency factor values are slightly smaller than the bond

vibrational frequencies could reflect a contribution to the reaction coordinate from other vibrational modes besides simple bond stretching, e.g. bond bending or molecular rotation.

Figure 5 illustrates the reaction coordinates that these data suggest might apply for proton and deuteron transmission through graphene. The activated complex energies are nearly the same for proton and deuteron, consistent with a structure in which O-H and O-D bonds are largely severed prior to proton / deuteron transmission. The difference in vibrational zero-point energies is the main factor responsible for differences in ion-transmission rates in this Figure. This situation is consistent with historical studies of hydrogen kinetic isotope effects on a wide range of reactions involving different degrees of bond breaking in the transition state. It is generally found that reactions in which bonds to hydrogen are mostly broken in the transition state give the largest primary hydrogen kinetic isotope effects.[24]

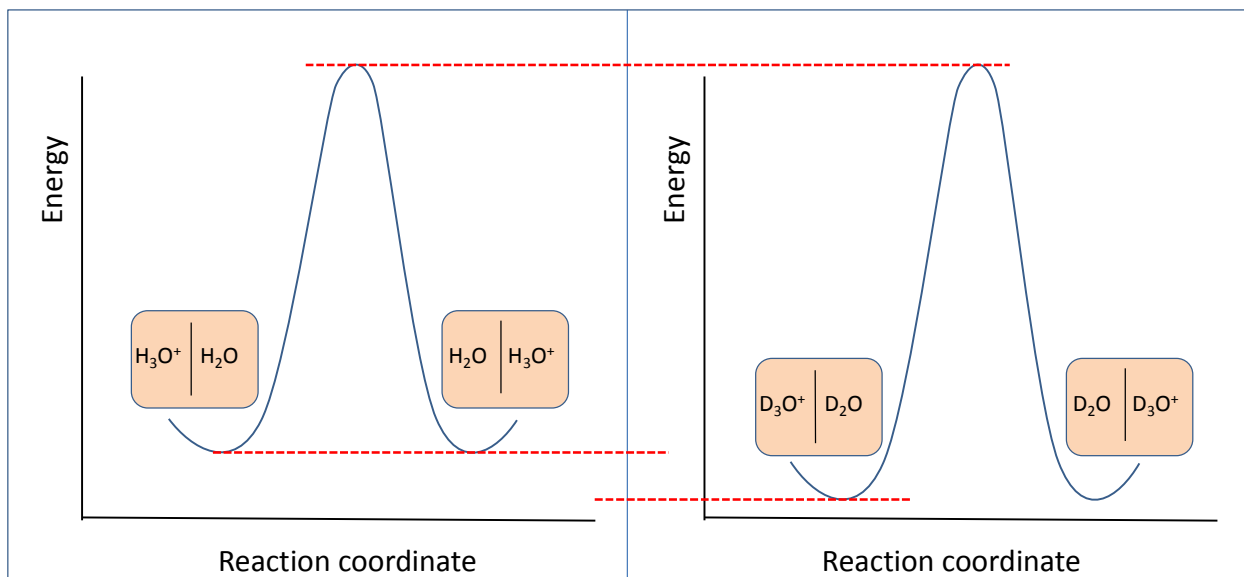


Figure 5. Illustrated reaction coordinates for proton and deuteron transmission through graphene, showing the role of zero-point energy in affecting the reaction rates and activation energies.

These findings provide input to ongoing experimental and computational studies of proton / deuteron transmission through graphene, insofar as they provide reliable values for both activation energies and absolute rates. Further experimental work could address the possible role of the energy required to transport protons from a bulk phase to the graphene surface. Such effects could formally be considered as double-layer effects in which a surface charge on graphene could play a highly significant role.[29] Proton concentration effects and local proton solvation effects in the double-layer region could also be important and will be the subject of ongoing studies. A possible role for proton / deuteron nuclear tunneling is also possible, as has been discussed recently.[30, 31] Nuclear tunneling could significantly change both the activation energy and the pre-factor in rate expressions. Detailed study of the graphene structure will also be important to evaluate the possible role of structural defects, even very rare defects that are difficult to detect spectroscopically, on proton / deuteron transmission.

4.0 Conclusions.

Interpretation of area-specific resistance values for proton / deuteron transmission through single-layer graphene leads to rate constants for **the** fundamental microscopic steps in the ion-transmission process. Interpretation of rate constants acquired over a range of temperatures between 30 and 60 C leads to activation energies and pre-exponential frequency factors for proton / deuteron transmission through graphene. Activation energies for both proton and deuteron transmission obtained from an Arrhenius analysis of these data are relatively low (approximately 50 kJ mole^{-1}) which is consistent with prior reports[5] and which informs ongoing efforts aimed at understanding the nature of the active sites where protons / deuterons pass through graphene. Frequency factors are relatively large, consistent with an ion-transmission mechanism that is largely adiabatic, with a transmission coefficient near 1.0.

5.0 Funding Sources.

We gratefully acknowledge the Office of Science, U.S. Department of Energy, through Grant DE-SC0018151 for financial support of the work.

REFERENCES

- [1] V. Berry, Impermeability of graphene and its applications, *Carbon*, 62 (2013) 1-10.
- [2] J.S. Bunch, S.S. Verbridge, J.S. Alden, A.M. van der Zande, J.M. Parpia, H.G. Craighead, P.L. McEuen, Impermeable atomic membranes from graphene sheets, *Nano Lett.*, 8 (2008) 2458-2462.
- [3] O. Leenaerts, B. Partoens, F.M. Peeters, Graphene: A perfect nanoballoon, *Appl. Phys. Lett.*, 93 (2008).
- [4] S. Bukola, Y. Liang, C. Korzeniewski, J. Harris, S. Creager, Selective proton / deuteron transport through Nafion | graphene | Nafion sandwich structures at very high current density, *J. Am. Chem. Soc.*, 140 (2018) 1743-1752.
- [5] S. Hu, M. Lozada-Hidalgo, F.C. Wang, A. Mishchenko, F. Schedin, R.R. Nair, E.W. Hill, D.W. Boukhvalov, M.I. Katsnelson, R.A.W. Dryfe, I.V. Grigorieva, H.A. Wu, A.K. Geim, Proton transport through one-atom-thick crystals, *Nature*, 516 (2014) 227-230.
- [6] M. Lozada-Hidalgo, S. Hu, O. Marshall, A. Mishchenko, A.N. Grigorenko, R.A.W. Dryfe, B. Radha, I.V. Grigorieva, A.K. Geim, Sieving hydrogen isotopes through two-dimensional crystals, *Science*, 351 (2016) 68-70.
- [7] M. Lozada-Hidalgo, S. Zhang, S. Hu, A. Esfandiari, I.V. Grigorieva, A.K. Geim, Scalable and efficient separation of hydrogen isotopes using graphene-based electrochemical pumping, *Nat. Commun.*, 8 (2017) 1-5.
- [8] J.L. Achtyl, R.R. Unocic, L.J. Xu, Y. Cai, M. Raju, W.W. Zhang, R.L. Sacci, I.V. Vlassiuk, P.F. Fulvio, P. Ganesh, D.J. Wesolowski, S. Dai, A.C.T. van Duin, M. Neurock, F.M. Geiger, Aqueous proton transfer across single-layer graphene, *Nat. Commun.*, 6 (2015).
- [9] M.I. Walker, P. Braeuninger-Weimer, R.S. Weatherup, S. Hofmann, U.F. Keyser, Measuring the proton selectivity of graphene membranes, *Appl. Phys. Lett.*, 107 (2015).
- [10] L. Tsetseris, S.T. Pantelides, Graphene: An impermeable or selectively permeable membrane for atomic species?, *Carbon*, 67 (2014) 58-63.
- [11] M. Miao, M.B. Nardelli, Q. Wang, Y.C. Liu, First principles study of the permeability of graphene to hydrogen atoms, *Phys. Chem. Chem. Phys.*, 15 (2013) 16132-16137.
- [12] L. Shi, A. Xu, G.H. Chen, T.S. Zhao, Theoretical Understanding of Mechanisms of Proton Exchange Membranes Made of 2D Crystals with Ultrahigh Selectivity, *J. Phys. Chem. Lett.*, 8 (2017) 4354-4361.
- [13] J.M.H. Kroes, A. Fasolino, M.I. Katsnelson, Density functional based simulations of proton permeation of graphene and hexagonal boron nitride, *Phys. Chem. Chem. Phys.*, 19 (2017) 5813-5817.
- [14] Q.J. Zhang, M.G. Ju, L. Chen, X.C. Zeng, Differential Permeability of Proton Isotopes through Graphene and Graphene Analogue Monolayer, *J. Phys. Chem. Lett.*, 7 (2016) 3395-3400.
- [15] M. Seel, R. Pandey, Proton and hydrogen transport through two-dimensional monolayers, *2D Materials*, 3 (2016).
- [16] Y.X. Feng, J. Chen, W. Fang, E.G. Wang, A. Michaelides, X.Z. Li, Hydrogenation Facilitates Proton Transfer through Two-Dimensional Honeycomb Crystals, *J. Phys. Chem. Lett.*, 8 (2017) 6009-6014.
- [17] J. Shetzline, S. Bukola, S.E. Creager, A convenient miniature test platform for polyelectrolyte membrane fuel-cell research, *J. Electroanal. Chem.*, 797 (2017) 8-15.

- [18] A.J. Bard, L.R. Faulkner, *Electrochemical Methods*, Second Edition, John Wiley & Sons, New York, 2001.
- [19] K.J. Oberbroeckling, D.C. Dunwoody, S.D. Minter, J. Leddy, Density of Nafion exchanged with transition metal complexes and tetramethyl ammonium, ferrous, and hydrogen ions: Commercial and recast films, *Anal. Chem.*, 74 (2002) 4794-4799.
- [20] R.A. Marcus, On the theory of ion transfer rates across the interface of two immiscible liquids, *J. Chem. Phys.*, 113 (2000) 1618-1629.
- [21] J.T. Hupp, M.J. Weaver, THE FREQUENCY FACTOR FOR OUTER-SPHERE ELECTROCHEMICAL REACTIONS, *J. Electroanal. Chem.*, 152 (1983) 1-14.
- [22] K.B. Wiberg, THE DEUTERIUM ISOTOPE EFFECT, *Chem. Rev.*, 55 (1955) 713-743.
- [23] R.P. Bell, RECENT ADVANCES IN STUDY OF KINETIC HYDROGEN ISOTOPE-EFFECTS, *Chem. Soc. Rev.*, 3 (1974) 513-544.
- [24] F.H. Westheimer, THE MAGNITUDE OF THE PRIMARY KINETIC ISOTOPE EFFECT FOR COMPOUNDS OF HYDROGEN AND DEUTERIUM, *Chem. Rev.*, 61 (1961) 265-273.
- [25] K.J. Laidler, M.C. King, THE DEVELOPMENT OF TRANSITION-STATE THEORY, *J. Phys. Chem.*, 87 (1983) 2657-2664.
- [26] Y. Marechal, INFRARED-SPECTRA OF WATER .1. EFFECT OF TEMPERATURE AND OF H/D ISOTOPIC DILUTION, *J. Chem. Phys.*, 95 (1991) 5565-5573.
- [27] J.J. Max, C. Chapados, Isotope effects in liquid water by infrared spectroscopy. III. H₂O and D₂O spectra from 6000 to 0 cm⁻¹, *J. Chem. Phys.*, 131 (2009).
- [28] M.E. Colvin, G.P. Raine, H.F. Schaefer, M. Dupuis, INFRARED INTENSITIES OF H₃O⁺, H₂DO⁺, HD₂O⁺, AND D₃O⁺, *J. Chem. Phys.*, 79 (1983) 1551-1552.
- [29] K. Li, Y. Tao, Z.W. Li, J.J. Sha, Y.F. Chen, Selective ion-permeation through strained and charged graphene membranes, *Nanotechnology*, 29 (2018).
- [30] J.W. Mazzuca, N.K. Haut, Theoretical description of quantum mechanical permeation of graphene membranes by charged hydrogen isotopes, *J. Chem. Phys.*, 148 (2018).
- [31] I. Poltavsky, L.M. Zheng, M. Mortazavi, A. Tkatchenko, Quantum tunneling of thermal protons through pristine graphene, *J. Chem. Phys.*, 148 (2018).